ELSEVIER

Journal of Molecular Structure: THEOCHEM 814 (2007) 113–117

THEO CHEM

www.elsevier.com/locate/theochem

Theoretical study of N–H···H–B blue-shifted dihydrogen bond

Yong Yang [a,*], Weijun Zhang [b]

[a] School of Materials Science and Chemical Engineering, Anhui Institute of Architecture and Industry, Hefei 230022, PR China
[b] Environmental Spectroscopy Laboratory, Anhui Institute of Optics and Fine Mechanics, Chinese Academy of Sciences, Hefei 230031, PR China

Received 7 February 2007; received in revised form 2 March 2007; accepted 2 March 2007
Available online 13 March 2007

Abstract

Theoretical calculations were performed to study the nature of the N–H···H–B blue-shifted dihydrogen bond in the complex BH_3NH_3···HNO. The geometric structures and vibrational frequencies of the complex BH_3NH_3···HNO at the MP2/6-31+G(d,p), MP2/6-311++G(d,p), B3LYP/6-31+G(d,p) and B3LYP/6-311++G(d,p) levels are calculated by standard and counterpoise-corrected methods, respectively. In the N–H···H–B dihydrogen bond, the calculated blue shift of N–H stretching frequency is in the vicinity of 130 cm^{-1}. From the natural bond orbital analysis it can be seen that the N–H bond length in the N–H···H–B dihydrogen bond is controlled by a balance of four main factors in the opposite directions: hyperconjugation, electron density redistribution, rehybridization and structural reorganization. Among them hyperconjugation has the effect of elongating the X–H bond, and the other three factors belong to the bond shortening effects. In the N–H···H–B dihydrogen bond, the shortening effects dominate which lead to the blue shift of the N–H stretching frequencies. In addition, solvent effect on the geometric structures, vibrational frequencies and interaction energies of the monomer and complex was studied in detail. It is relevant to the relatively dielectric constants (ε).

Keywords: Blue-shifted hydrogen bond; Dihydrogen bond; Hyperconjugation; Rehybridization; Electron density redistribution; Structural reorganization

1. Introduction

Unconventional hydrogen bonds (H-bond) are often a subject of investigation [1,2] since they play an important role in many biochemical processes, in crystal engineering, chemical catalysis, etc. The unusual phenomenon of ''blue-shifted'' or ''improper'' X–H···Y hydrogen bonds continues to receive significant experimental and theoretical attention [3–20], mainly due to the pioneering work by Hobza and Havlas [3,4]. Blue-shifted hydrogen bonds X–H···Y are characterized by a contraction of the X–H bond and a blue shift of the X–H stretching frequency, which are in sharp contrast to those rooted to the conventional hydrogen bonds.

Recently, another type of unconventional hydrogen bond has also attracted considerable attention. The new term dihydrogen bond was coined to describe this hydridic-to-protonic interaction of the type X–H···H–E, where X–H is the typical proton-donating bond (such as O–H or N–H) and E designates a transition metal or boron [21–23]. To the best of our knowledge, the X–H···H–E blue-shifted dihydrogen bond was scarcely reported [24]. It may be of interest to make a comparison between the X–H···Y blue-shifted hydrogen bond and the X–H···H–E blue-shifted dihydrogen bond. Then, we believe that this study on the X–H···H–E blue-shifted dihydrogen bond is valuable and interesting. One goal of this article is to find case of the X–H···H–E blue-shifted dihydrogen bond.

The complexes $(BH_3NH_3)_2$ and BH_3NH_3···NH_3 have been theoretically studied [23]. They showed that the N–H···H–B red-shifted dihydrogen bonds were formed in these complexes. In this article, we study the interesting N–H···H–B blue-shifted dihydrogen bonds in the complexes BH_3NH_3···HNO. Our next goal of this article is expected to provide a reasonable explanation about the origins of the blue-shifted dihydrogen bonds. Hence the study

* Corresponding author. Tel.: +86 551 3828100; fax: +86 551 3828106.
E-mail addresses: yongyang@aiai.edu.cn, yongyang@aiofm.ac.cn (Y. Yang).

0166-1280/$ - see front matter © 2007 Elsevier B.V. All rights reserved.
doi:10.1016/j.theochem.2007.03.005

may provide novel and important insights into the mechanism of the blue-shifted dihydrogen bonds.

2. Computational methods

The geometric structures and vibrational frequencies of the complex $BH_3NH_3\cdots HNO$ were investigated using both standard and counterpoise-corrected(CP) [25,26] optimization at the MP2/6-31+G(d,p), MP2/6-311++G(d,p), B3LYP/6-31+G(d,p) and B3LYP/6-311++G(d,p) levels, respectively. The basis set superposition errors (BSSE) were calculated according to the counterpoise method proposed by Boys and Bernardi [26]. In addition, the partial optimization on the HNO monomer was performed at MP2/6-311++G(d,p) and B3LYP/6-311++G(d,p) levels. According to Onsager model, the SCRF calculations on the HNO monomer and complex $BH_3NH_3\cdots HNO$ were carried out at B3LYP/6-31+G(d,p) level. Natural bond orbital (NBO) [27] analysis was performed at the MP2/6-311++G(d,p) level. All the calculations are performed using the Gaussian 03 program packages [28].

3. Results and discussion

3.1. Geometries, frequencies and energies

The optimized structures of the monomers and complex are described in Fig. 1. The geometric characteristics, vibrational frequencies and interaction energies of the monomers and complex determined by both standard and CP optimizations at MP2/6-31+G(d,p), MP2/6-311++G(d,p), B3LYP/6-31+G(d,p) and B3LYP/6-311++G(d,p) levels are presented in Tables 1 and 2. As depicted in Fig. 1, there is an N–H···O hydrogen bond and two N–H···H–B dihydrogen bonds in the complex $BH_3NH_3\cdots HNO$ simultaneously, forming cyclic structure. For the complex $BH_3NH_3\cdots HNO$, the bond length and vibrational frequencies of N2–H1 obtained by MP2 method agrees well with that obtained by B3LYP method. According to the basis sets effect, it can be seen that there is inconspicuous effect on the optimized structures. Owning to the existence of BSSE, the interaction energies are overestimated by the standard calculations [25]. In order to eliminate this effect, the CP-corrected calculations were performed. Compared to the standard calculations, the H1···H6(7) and O3···H8 distances obtained by CP-corrected calculations are obviously longer.

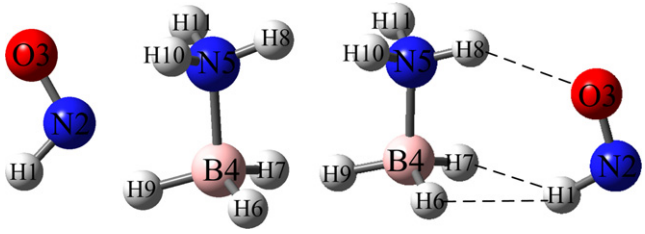

Fig. 1. Optimized structure of the monomers and complex.

As shown in Tables 1 and 2, it becomes evident that there are contractions of N2–H1 bond compared to the HNO monomer, employing the standard and CP calculations. As far as the H-bond type prediction is concerned, all results indicate N2–H1 stretching frequencies are blue-shifted in the complex $BH_3NH_3\cdots HNO$. On the basis of these analyses, it can be confirmed that the complex $BH_3NH_3\cdots HNO$ possesses two blue-shifted dihydrogen bonds: N2–H1···H6–B4 and N2–H1···H7–B4. It should be pointed out that N2–H1 stretching frequencies display very large blue shifts. All calculations show the blue shifts are up to 140 cm^{-1} at most and up to 124 cm^{-1} at least.

The intermolecular interaction energies with both BSSE correction and ZPE correction were listed in Tables 1 and 2. As shown in Tables 1 and 2, the BSSE corrected and ZPE corrected energies are relatively large. The results indicate that BSSE correction and ZPE correction are important to accurately describe the intermolecular interaction energies.

3.2. NBO analysis

In order to investigate the mechanism on the blue-shifted dihydrogen bonds, the NBO analysis was performed at MP2/6-311++G(d,p) level and the corresponding results were listed in Table 3. The NBO analysis results for the monomers suggest that in HNO the H atom carries a significant amount of positive charge. On the other hand, in BH_3NH_3 the H6(7) atoms carry a certain amount of negative charge. Therefore, hydridic-to-protonic interaction should take place in the complex

Table 1
The partial parameters of optimized complex at MP2 /6-31+G(d,p), MP2/6-311++G(d,p) level

		MP2 /6-31+G(d,p)		MP2/6-311++G(d,p)	
		Standard	CP	Standard	CP
$BH_3NH_3\cdots HNO$	r(H1···H6)/Å	2.1849	2.2508	2.1831	2.2418
	r(O3···H8)/Å	2.1586	2.2274	2.1569	2.2293
	Δr(N2–H1)/Å	−0.0061	−0.0063	−0.0069	−0.0068
	Δv(N2–H1)/cm^{-1}	+125	+124	+132	+128
	ΔE/kcal mol^{-1}	−8.13	−8.06	−7.86	−7.80
	ΔE^{CP}/kcal mol^{-1}	−6.59	−6.66	−6.46	−6.53
	$\Delta E^{CP,\ ZPE}$/kcal mol^{-1}	−4.75	−4.85	−4.68	−4.76

Table 2
The partial parameters of optimized complex at B3LYP /6-31+G(d,p), B3LYP/6-311++G(d,p) level

		B3LYP /6-31+G(d,p)		B3LYP/6-311++G(d,p)	
		Standard	CP	Standard	CP
$BH_3NH_3\cdots HNO$	r(H1···H6)/Å	2.1683	2.1806	2.1796	2.1934
	r(O3···H8)/Å	2.1091	2.1439	2.1205	2.1463
	Δr(N2–H1)/Å	−0.0071	−0.0072	−0.0083	−0.0082
	Δv(N2–H1)/cm^{-1}	+128	+129	+140	+139
	ΔE/kcal mol^{-1}	−7.23	−7.22	−7.03	−7.02
	ΔE^{CP}/kcal mol^{-1}	−6.59	−6.69	−6.49	−6.61
	$\Delta E^{CP,ZPE}$/kcal mol^{-1}	−4.78	−4.87	−4.67	−4.81

Table 3
NBO analysis of the monomer and complex at MP2/6-311++G(d,p) level

	BH_3NH_3	HNO	$BH_3NH_3\cdots HNO$
$E^{(2)}\sigma$(B4–H6) → σ^*(N2–H1)/kcal mol^{-1}		–	1.00
$E^{(2)}\sigma$(B4–H7) → σ^*(N2–H1)/kcal mol^{-1}		–	1.00
$E^{(2)}$ n_2(O3) → σ^*(N2–H1)/kcal mol^{-1}		18.63	14.65
R-index [N2–H1···H7(H6)–B4]		–	1.99
σ^*(N2–H1)/e		0.03034	0.02636
$\Delta\sigma^*$(N2–H1)/e		–	−0.00398
q(H6)	−0.10816		
q(H1)/e		0.25866	0.31144
ΔqH1)/e		–	0.05278
spn(N2–H1)		sp4.07	sp3.52
% s-char(N2–H1)		19.72%	22.06%
pol N2%		63.97%	66.50%
(σ_{N9-H8}), H1%		36.03%	33.50%

$BH_3NH_3\cdots HNO$. This means that the non-covalent interaction involved in N–H···H–B can be defined as dihydrogen bond. In the NBO analysis, the importance of hyperconjugative interaction and electron density transfer (EDT) from σ(E–H) to σ^*(X–H) in the X–H···H–E dihydrogen bond is well known, which leads to an increase in population of X–H antibonding orbital. The increase of electron density in X–H antibonding orbital weakens the X–H bond, which leads to its elongation and concomitant red shift of X–H stretching frequency. In general, the larger the hyperconjugative σ(E–H) → σ^*(X–H) interaction, the larger the electron density increase in the σ^*(X–H), and the X–H bond length elongation becomes more obvious. From Table 3, the hyperconjugative σ(B4–H6) → σ^*(N2–H1) and σ(B4–H7) → σ^*(N2–H1) interactions in the complex are 1.00 kcal/mol, which contribute to the electron density increase in the σ^*(N2–H1). However, the electron density in the σ^*(N2–H1) decreased instead of increasing. We pay more attention to phenomenon which is the electron density decrease in the σ^*(N2–H1). Hobza and colleagues showed that reason for the electron density decrease in the σ^*(X–H) is electron density redistribution effect [6,7]. Recently, it has been reported that the change of electron density in the σ^*(X–H), compared with monomer, is a combination of two effects for the Z–X–H···Y (or H–E) H-bond [19,20]. In the type Z–X–H···Y (or H–E) H-bond, where Z is an electronegative atom having one and more lone electron pairs (such as F, O, N), the hyperconjugative n(Y) or σ(E–H) → σ^*(X–H) interaction leads to an increase of electron density in the σ^*(X–H). In contrast, a decrease in the n(Z) → σ^*(X–H) interaction of the complex, relative to the monomer, has the opposite effect. On the basis of electron density redistribution effect, we define a novel index, called R-index, which can be determined as a ratio of the variable magnitude of the n(Z) → σ^*(X–H) interaction and the magnitude of the n(Y) or σ(E–H) → σ^*(X–H) interaction in the Z–X–H···Y (or H–E) system. Here, the R-index can be expressed as

$$R\text{-index} = \frac{E_{\text{monomer}}[n(\text{Z}) \rightarrow \sigma^*(\text{X–H})] - E_{\text{complex}}[n(\text{Z}) \rightarrow \sigma^*(\text{X–H})]}{E[n(\text{Y}) \text{ or } \sigma(\text{E–H}) \rightarrow \sigma^*(\text{X–H})]} \quad (1)$$

where the $E_{\text{monomer}}[n(\text{Z}) \rightarrow \sigma^*(\text{X–H})]$ and $E_{\text{complex}}[n(\text{Z}) \rightarrow \sigma^*(\text{X–H})]$ mean the n(Z) → σ^*(X–H) interactions in the monomer and the complex, respectively. The E[n(Y) or σ(E–H) → σ^*(X–H)] denotes the n(Y) or σ(E–H) → σ^*(X–H) interaction in the complex. According to the definition of the R-index, the R-index can be used to describe the strength of the electron density redistribution. In general, the larger the value of R-index is, the stronger the electron density redistribution effect is. As shown in Table 3, the magnitude of n(O3) → σ^*(N2–H1) interactions have an evident change relative to the HNO monomer. Furthermore, the value of the R-index (B4–H6···H1–N2) is relatively large and attains to 1.99, which indicates that the electron density redistribution effect is very significant in the B4–H6(7)···H1–N2 dihydrogen bonds. Therefore, the electron density redistribution exceeds the hyperconjugation in the B4–H6(7)···H1–N2 dihydrogen bonds, which leads to the electron density decrease in the σ^*(N2–H1). It makes the N2–H1 bond contract and is contributed to blue shift of N2–H1 stretching frequency. To this point, the NBO results fully interpret the electron density decrease in the σ^*(N2–H1) with respect to that in the monomer HNO.

Alabugin et al. [18] have recently proposed that rehybridization is the main factor for the H-bond blue shifts. In their opinion, the positive charge of the H atom in the X–H···Y hydrogen bonds is more than that in the monomer; according to Bent's rule, rehybridiza-

tion increases the s-character of X–H bond, strengthen its polarization, and consequently, shorten the X–H bond. Seen from Table 3, our results coincide well with the results of rehybridization. In the complex $BH_3NH_3\cdots HNO$, the positive charge on the H atom of N2–H1 increases, so do the s-character of the hybrid orbital in N2–H1 and the polarization, which contributes to the N2–H1 contraction.

3.3. Structural reorganization

Hobza and Havlas [3] proposed that there was difference in nature between the red-shifted and blue-shifted hydrogen bonds and the structural reorganization is the fundamental reason for the blue-shifted H-bond. For the normal X–H$\cdots$Y red-shifted hydrogen bond, electron transfers from the lone pair electron of electron donator to the σ^*(X–H) of the electron acceptor, which elongates the X–H bond and leads to a red shift. For the blue-shifted hydrogen bond, there are two steps in the process. First, owning to hyperconjugation, the electron is transfered to the other parts of the electron acceptor, which elongates the other bonds of the acceptor. Second, the electron acceptor undergoes a structural reorganization which contributes to the X–H contraction and blue shift of stretching frequency. As listed in Table 4, the bond length of N2–O3 in HNO is evidently elongated in the complex $BH_3NH_3\cdots HNO$. In order to deepen the understanding of the structural reorganization effect on the blue shift of N–H bond, the partial optimization on the HNO monomer was performed at B3LYP/6-311++G(d,p) and MP2/6-311++G(d,p) levels. In the process, we optimized the HNO monomer with an elongated N–O bond taken from the optimized complex, and this bond was kept frozen during the optimization. The results in Table 4 show that N2–O3 bond elongation can only lead to a small contraction in bond length and a slight blue shift in stretching frequencies of N2–H1. For the complex, at the MP2/6-311++G(d,p) level the blue shift is up to 132 cm^{-1}, while it is only 22 cm^{-1} due to the structural reorganizations. Therefore, we can exclude the possibility of the structural reorganization being the fundamental reason for the blue-shifting dihydrogen bond.

3.4. Solvent effect on the structures, frequencies and interaction energies

In order to investigate the solvent effect on the structures, frequencies and interaction energies of monomer and complex, the SCRF calculations were performed on the monomer and complex at B3LYP/6-31+G(d,p) level (the relatively dielectric constants are 2.23, 8.93, 24.55, 32.63, 36.64 and 78.39, respectively). The corresponding results are summarized in Table 5. It is clear from the change of bond lengths given in Table 5 that solvent effect leads to decrease of the N2–H1 bond length in the monomer HNO. This behavior is more evident as ε is below 10.0. For the complex $BH_3NH_3\cdots HNO$, the solvent effect on the structure is not significant. With the increase of ε, the H1$\cdots$H6 distance shows a slight contraction while the O3$\cdots$H8 distance is a small elongation. The N2–H1 bond length is almost independent of ε in the complex $BH_3NH_3\cdots HNO$. As shown in Table 5, the solvent effects have a different influence on the geometries of the complex $BH_3NH_3\cdots HNO$ and the monomer HNO. As a result, the blue shift of the N2–H1 stretching frequency decreases as ε increases. At the B3LYP/6-31+G(d,p) level, the N2–H1 blue shift is up to128 cm^{-1} in the gas phase and 71 cm^{-1} in the liquid ($\varepsilon = 78.39$). In addition, we notice that the interaction energies in the complex $BH_3NH_3\cdots HNO$ show a decrease with ε increasing.

Table 4
The change between the partial optimized HNO and all optimized HNO of the bond lengths (N2–H1) and stretching frequencies at B3LYP/6-311++G(d,p) and MP2/6-311++G(d,p) levels

		B3LYP /6-311++G(d,p)		MP2/6-311++G(d,p)	
		Standard	CP	Standard	CP
$BH_3NH_3\cdots HNO$	Δr(N2–O3)/Å	+0.0083	+0.0079	+0.0060	+0.0050
	Δr((N2–H1)/Å	−0.0021	−0.0020	−0.0016	−0.0014
	Δv(N2–H1)/cm^{-1}	+28	+27	+22	+19

Table 5
Partial optimized parameters of HNO monomer and complex in different solvents at B3LYP/6-31+G(d, p) levels

		$\varepsilon = 2.23$	$\varepsilon = 8.93$	$\varepsilon = 24.55$	$\varepsilon = 32.63$	$\varepsilon = 36.64$	$\varepsilon = 78.39$
HNO	r(N2–H1)/Å	1.0622	1.0609	1.0606	1.0606	1.0605	1.0605
$BH_3NH_3\cdots HNO$	r(N2–H1)/Å	1.0566	1.0565	1.0564	1.0564	1.0564	1.0564
	r(O3$\cdots$H8)/Å	2.1616	2.2316	2.2579	2.2623	2.2639	2.2708
	r(H1$\cdots$H6)/Å	2.1332	2.0994	2.0895	2.0879	2.0874	2.0852
	Δr(N2–H1)/Å	−0.0056	−0.0044	−0.0042	−0.0042	−0.0041	−0.0041
	Δv(N2–H1)/cm^{-1}	+101	+79	+73	+72	+72	+71
	ΔE/kcal mol^{-1}	−5.04	−2.96	−2.41	−2.33	−2.30	−2.18

4. Conclusions

The complex $BH_3NH_3\cdots HNO$ has been investigated with both standard and counterpoise-corrected optimization methods at the MP2/6-31+G(d,p), MP2/6-311++G(d,p), B3LYP/6-31+G(d,p) and B3LYP/6-311++G(d,p) levels, respectively. The complex $BH_3NH_3\cdots HNO$ exhibits simultaneously two N2–H1$\cdots$H6(7)–B4 blue-shifted dihydrogen bonds and an N5-H8$\cdots$O3 red-shifted hydrogen bond. The calculations show that the N2–H1 stretching frequency displays a very large blue shift (about 130 cm^{-1}). This value of blue shift is the largest for the X–H$\cdots$H–E dihydrogen bond as reported in the literature so far. For the N2–H1$\cdots$H6(7)–B4 blue-shifted dihydrogen bonds, NBO analysis fully interprets the electron density decrease in the σ^*(N2–H1) due to existence of the significant electron density redistribution effect. Furthermore, we can conclude that the unusual blue-shifted dihydrogen bond is duo to an intricate combination of three bond shortening effects: electron density redistribution, rehybridization and structural reorganization.

Acknowledgements

This work is supported by the National Natural Science Foundation of China (G20477043) and Knowledge Creative Program by Chinese Academy of Sciences (KJCX2- 08).

References

[1] R. Sumathi, A.K. Chandra, Chem. Phys. Lett. 271 (1997) 287.
[2] S.J. Grabowski, Chem. Phys. Lett. 327 (2000) 203.
[3] P. Hobza, Z. Havlas, Chem. Rev. 100 (2000) 4253.
[4] P. Hobza, Z. Havlas, Chem. Phys. Lett. 303 (1999) 447.
[5] S.N. Delanoye, W.A. Herrebout, B.J. van der Veken, J. Am. Chem. Soc. 124 (2002) 11854.
[6] J. Chocholoušová, V. Špirko, P. Hobza, Phys. Chem. Chem. Phys. 6 (2004) 37.
[7] P. Hobza, V. Špirko, Phys. Chem. Chem. Phys. 5 (2003) 1290.
[8] A. Karpfen, E.S. Kryachko, J. Phys. Chem. A 107 (2003) 9724.
[9] A. Karpfen, E.S. Kryachko, Chem. Phys. 310 (2005) 310.
[10] A. Karpfen, J. Mol. Struct. (Theochem) 710 (2004) 85.
[11] S.A.C. McDowell, J. Chem. Phys. 119 (2003) 3711.
[12] S.A.C. McDowell, Phys. Chem. Chem. Phys. 5 (2003) 808.
[13] H. Matsuura, H. Yoshida, M. Hieda, S. Yamannaka, T. Harada, K. Shin-ya, K. Ohno, J. Am. Chem. Soc. 125 (2003) 13910.
[14] S. Scheiner, T. Kar, J. Phys. Chem. A 106 (2002) 1784.
[15] X.S. Li, L. Liu, H.B. Schlegel, J. Am. Chem. Soc. 124 (2002) 9639.
[16] K. Hermansson, J. Phys. Chem. A 106 (2002) 4695.
[17] A. Masunov, J.J. Dannenberg, R. Contreras, J. Phys. Chem. A 105 (2001) 4737.
[18] I.V. Alabugin, M. Manoharan, S. Peabody, F. Weinhold, J. Am. Chem. Soc. 125 (2003) 5973.
[19] Y. Yang, W.J. Zhang, X.M. Gao, Int. J. Quantum Chem. 106 (2006) 1199.
[20] Y. Liu, W.Q. Liu, Y. Yang, J.G. Liu, Int. J. Quantum Chem. 106 (2006) 2122.
[21] R. Custelcean, J.E. Jackson, Chem. Rev. 101 (2001) 1963.
[22] S.J. Grabowski, W.A. Sokalski, J. Leszczynski, J. Phys. Chem. A 108 (2004) 5823.
[23] T. Kar, S. Scheiner, J. Chem. Phys. 119 (2003) 1473.
[24] Y. Feng, S.W. Zhao, L. Liu, J.T. Wang, X.S. Li, Q.X. Guo, J. Phys. Org. Chem. 17 (2004) 1099.
[25] S. Simon, M. Duran, J.J. Dannenbery, J. Chem. Phys. 105 (1996) 11024.
[26] S.F. Boys, F. Bernardi, Mol. Phys. 19 (1970) 553.
[27] A.E. Reed, L.A. Curtiss, F. Weinhold, Chem. Rev. 88 (1988) 899.
[28] M.J. Frisch et al., Gaussian 03, Revision B. 02, Gaussian, Inc., Pittsburgh, PA, 2003.